Journal of Innovative Optical Health Sciences
Vol. 8, No. 1 (2015) 1540003 (11 pages)

DOI: 10.1142/S1793545815400039

World Scientific
www.worldscientific.com

Anti-tumor activities of a novel chlorin derivative for photodynamic therapy *in vitro* and *in vivo*

Li-Jun Zhang*, Lai-Xing Wang†, Wei-Li Zhang*, Yi-Jia Yan* and Zhi-Long Chen*,‡

*Department of Pharmaceutical Science & Technology
College of Chemistry and Biology, Donghua University
Shanghai 201620, P. R. China

†Changhai Hospital, Second Military Medical University
Shanghai 200433, P. R. China
‡zlchen1967@yahoo.com

Received 30 October 2013
Accepted 5 January 2014
Published 20 February 2014

In this study, a novel photosensitizer meso-tetra (3-pyrrolidinomethyl-4-methoxyphenyl) chlorin (TPMC) was reported. It displays a characteristic long wavelength absorption peak at 656 nm and it shows a singlet oxygen quantum yield of 0.48. After light irradiation with 650 nm laser, it can kill Eca-109 and SMMC-7721 cells *in vitro* (25 mW/cm^2, 1.2 to 3.6 J/cm^2) and destroy Eca-109 tumor in nude mice (50 mW/cm^2, 90 J/cm^2). It has the perspective to be developed as a new anti-tumor drug in photodynamic therapy (PDT) photodiagnosis, and deserves further investigation.

Keywords: TPMC; chlorin; tumor; photosensitizer; photodynamic therapy.

1. Introduction

Photodynamic therapy (PDT) is emerging as a promising method for the treatment of a variety of oncological, dermatological, cardiovascular and ophthalmic diseases.[1–6] PDT destroys target cells in the presence of oxygen when light irradiates a photosensitizer, generating highly reactive singlet oxygen and/or other reactive oxygen species (ROS) such as superoxide ion and hydroxyl radicals. ROS then attack biological targets, causing destruction through direct cellular damage, vascular shutdown and activation of an immune response against targeted cells.[7]

Photosensitizers in PDT play a critical role.[8,9] Selection of an appropriate photosensitizer is of paramount importance for PDT.[10] Factors that may influence the selection include conjugation compatibility and yield, quencher compatibility, photosensitizer hydrophobicity, excitation profile, singlet oxygen quantum yield, fluorescence quantum yields and photosensitizer dark toxicity.[3]

Chlorin-based photosensitizers have been found to have applications as phototoxic drugs for PDT.[11–14] They are often selected because of their high singlet oxygen quantum yields and spectroscopic properties[15]: Characteristic absorption spectra with a Soret band at approximately 415 nm and a usually narrow but very strong Q-band around 650 nm, with a molar absorption coefficient in the range of 10^5 $M^{-1}\,cm^{-1}$. Temoporfin and meso-tetahydroxyphenylchlorin have been used for esophageal cancer, head and neck cancer, early gastric cancer and gastrointestinal cancer superficial portion.[16–18]

We herein report the photobiological studies of a novel Chlorin-based compound meso-tetra (3-pyrrolidinomethyl-4-methoxyphenyl) chlorin (TPMC) (see Fig. 1) using human esophageal cancer cells (Eca-109) and human hepatocellular carcinoma cells (SMMC-7721) *in vitro* and *in vivo*. The photophysical and photochemical properties have been evaluated. Our results show the efficiency of TPMC for suitable PDT applications. To further elucidate the cellular mechanism of action, the intracellular localization was tested for the purpose of determining the primary photodamage site.

2. Experimental Section

2.1. *Materials*

TPMC (see Fig. 1) was synthesized in our laboratory and is being applied for patent. All other chemicals and reagents were of analytical grade and used without any purification.

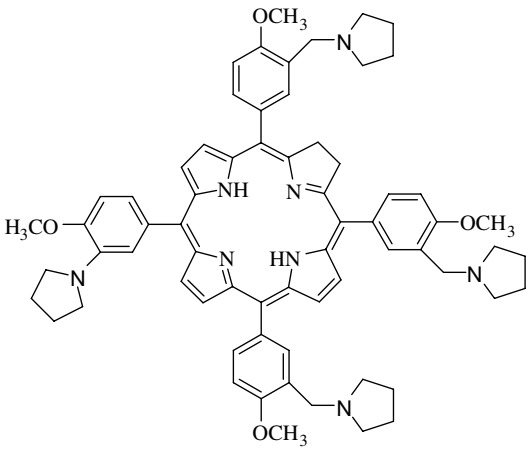

Fig. 1. Chemical structure of TPMC in DMF.

2.2. *Absorption and emission spectra*

UV-Vis absorption spectrum was recorded on an ultraviolet visible spectrophotometer (Model V-530, Japan). Fluorescence spectra were measured on a Fluorescence Spectrometer (FluoroMax-4, France). Slits were kept narrow to 1 nm in excitation and 1 or 2 nm in emission. Right angle detection was used. All the measurements were carried out at room temperature in quartz cuvettes with path length of 1 cm. TPMC was dissolved in N, N-dimethylformamide (DMF) to get 5 μM solution.

2.3. *Singlet oxygen quantum yield*

DPBF was used as a $^1O_2$ trapping reagent in DMF solution. In a typical experiment, 2 mL DMF solution containing 20 μM 1,3-diphenylisobenzofuran (DPBF) and 0.5 μM TPMC was placed in a sealed quartz cuvette. A 5 mW Nd:YAG laser (650 nm) was used as the light source. The absorbance of the solution at 410 nm was measured every 10 s for a 120 s period with an ultraviolet visible spectrophotometer.[19] The decrease of the absorbance caused by photobleaching of DPBF was measured and corrected in all experiments. The natural logarithm values of absorption of DPBF at 410 nm were plotted against the irradiation time and fit by a first-order linear least-squares model to get the singlet oxygen generation rate of the photosensitized process.[20] The $^1O_2$ quantum yield of TPMC in DMF was calculated using Methylene blue as a standard.

2.4. *In vitro experiments*

2.4.1. *Cell lines and culture conditions*

Human esophageal cancer cell line (Eca-109) and human hepatocellular carcinoma cell line (SMMC-7721) were obtained from the Type Culture Collection of the Chinese Academy of Sciences. All cell culture related reagents were purchased from Shanghai Ming Rong Bio-Science Technology Co., Ltd. Cell lines were maintained in normal RPMI-1640 culture medium with 10% fetal bovine serum (FBS) and 100 IU/mL penicillin and 100 μg/mL streptomycin. Both cell lines were kept in a CO_2 incubator with 5% CO_2 and 100% relative humidity at 37°C.

2.4.2. *Cellular uptake*

Eca-109 and SMMC-7721 cells (1×10^4 cells/well) were grown overnight at 37°C in 96-well cell culture

plates. A 5 μM solution of TPMC in culture medium with 4% serum was then exposed to cells from 30 min to 24 h in the dark, respectively. The solution was prepared by diluting the stock solution (10 mM) in dimethyl sulfoxide (DMSO) with proper cell culture medium to the desired final concentration (5 μM). The highest DMSO concentration did not exceed 0.3% v/v. After incubation, cells were washed three times with PBS and solubilized in 100 μL/well DMSO. Drug cellular uptake was measured by determining the fluorescence emission of TPMC with a Spectrofluorometer (FluoroMax-4, France) at 420 nm excitation and 656 nm emission wavelengths. Results were expressed as the emission relative to the total number of cells.

2.4.3. *Toxicity in the dark*

Eca-109 and SMMC-7721 cells (1×10^4 cells/well) grown in 96-well cell culture plates were incubated for 24 h with concentration from 2 to 10 μM of TPMC. The solutions were prepared as described above. Maximum DMSO concentration in the cell culture medium was $< 0.3\%$ v/v. Cell toxicity analysis was performed at the end of the incubation time. Briefly, 3-(4,5-Dimethylthiazol-2-yl)-2,5-diphenyltetrazolium bromide (MTT) dissolved in phosphate buffered saline (PBS) (5 mg/mL) was added (10 μL per 100 μL of medium) to all wells and the plates were incubated at 37°C with 5% CO^2 and 100% relative humidity for 4 h. After this time, the medium was then discarded and 150 μL DMSO was added to each well according to the method of Alley *et al.*[35] The MTT test was performed using an ELISA plate reader at 570 nm (Bio-Rad, California, USA).

2.4.4. *Phototoxicity*

Cells were prepared as described above. Thereafter, the media containing TPMC were replaced with drug-free medium containing 10% of serum and cells were irradiated at 650 nm at a fluence rate of 25 mW/cm^2 and light doses ranging from 1.2 to 3.6 J/cm^2. This wavelength was emitted by a Nd:YAG laser. Control experiments performed in the absence of any photosensitizer indicated that light doses up to 3.6 J/cm^2 caused no evident cell damage. A plate similarly treated but not exposed to light was used as reference for the dark cytotoxicity in the same experimental conditions. Experiments were conducted in quadruplicate and repeated thrice. Analysis of cell phototoxicity using the MTT assay as described above was performed after a further incubation of 24 h after irradiation and compared to the values of control cells without light irradiation.

2.4.5. *Intracellular localization*

Eca-109 and SMMC-7721 cells grown on coverslips were incubated with the solution (5 μM) of TPMC for 4 h at 37°C in the dark. Then after removing the solution with PBS, cells were stained with fluorescent dye (Hoechst 33342) for cell nucleus diluted in the culture medium without serum. After washing with PBS, coverslips were fixed for 10 min at −4°C with 4% paraformaldehyde and cells were then examined by fluorescence with a confocal microscopy (LSM 410, Zeiss, Germany). TPMC was excited at 420 nm and its emission was monitored at wavelengths 656 nm, and Hoechst 33342 was excited at 350 nm and blue fluorescence was detected at 461 nm.

2.5. *In vivo experiments*

2.5.1. *Animal models*

TPMC was evaluated in nude mice (10 mice/group) bearing Eca-109 tumors, implanted subcutaneously, and the tumors were allowed to grow to an approximate diameter of 5–7 mm.

2.5.2. *In vivo PDT efficacy*

When the tumor reached 5–7 mm in diameter, the mice were injected with TPMC at a dose of 8 μM. At 24 h post-injection, the mice were restrained in plastic plexiglass holders without anesthesia and treated with laser light (650 nm, 90 J/cm^2, 50 mW/cm^2). The power was monitored during the entire treatment. Post-PDT, the mice were observed daily for tumor regrowth or tumor cure. Visible tumors were measured using two orthogonal measurements L and W (perpendicular to L), and the volumes were calculated using the Microsoft Excel formula $V = LW^2/2$ and recorded. Mice were considered as cured if there was no palpable tumor by day 60–90. Once the tumor reached 400 mm^3, the mice were euthanized due to tumor burden as per RPCI IACUC rules.

3. Results

3.1. *UV-Vis absorption spectrum*

UV-Vis absorption spectrum was recorded on a standard commercial spectrophotometer. The absorption

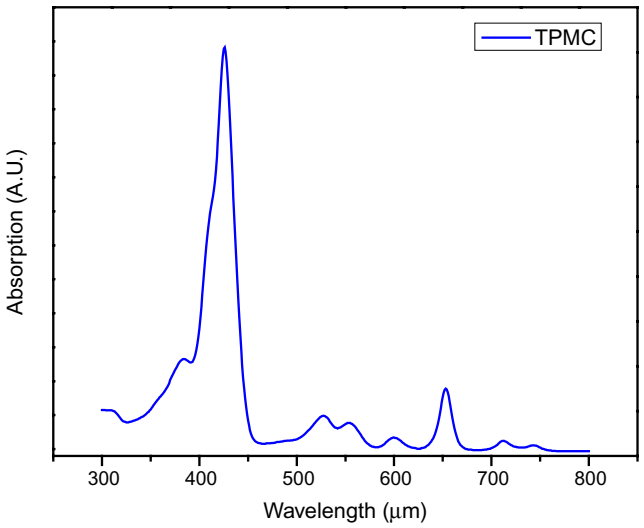

Fig. 2. UV-Vis absorption spectrum of TPMC in DMF. Its maximum absorbance is at 420 nm, and at 527, 552, 600, 653 and 712 nm, also it has absorption.

Table 1. Molar absorption coefficients of TPMC.

Wavelength (nm)	Molar absorption coefficient $\varepsilon(\mathrm{M}^{-1}\cdot\mathrm{cm}^{-1})$
527	9091
552	7142
600	3703
653	16,667
712	2857

peak of TPMC in DMF is at 420 nm, and it also has absorption at 527, 552, 600, 653 and 712 nm (see Fig. 2). Molar absorption coefficients of TPMC are shown in Table 1.

3.2. *Fluorescence spectrum*

Fluorescence spectra were measured using spectrofluorimeter described in Sec. 2. TPMC can be excited at 420 nm, and its emission was monitored at wavelengths 656 nm (see Fig. 3).

3.3. *Singlet oxygen quantum yield*

Energy transfer between the triplet state of photosensitizers and ground state molecular oxygen leads to the production of singlet oxygen. There is an essentiality of high efficiency of transfer of energy between excited triplet state of TPMC and ground state of oxygen to generate large amounts of singlet oxygen, necessary for PDT.

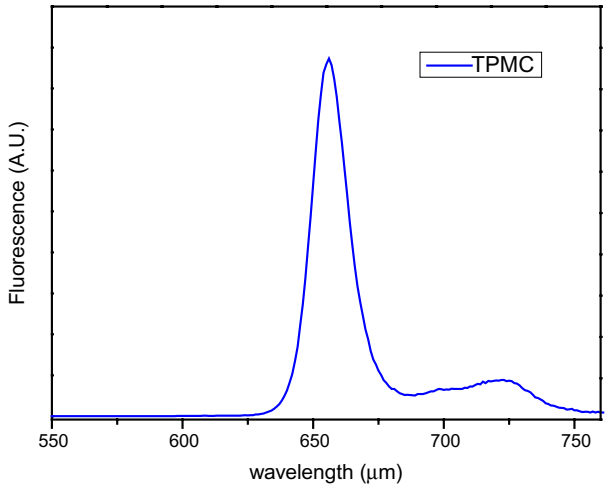

(a)

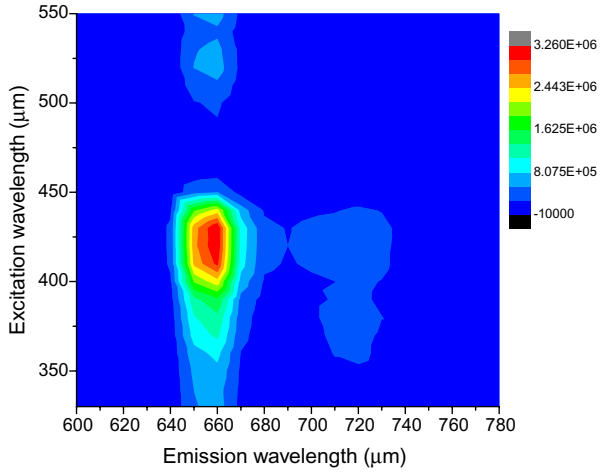

(b)

Fig. 3. Emission spectrum and excitation and emission spectra matrix of TPMC in DMF. (a) Emission spectrum of TPMC, which was excited at 420 nm, and its peak was at 656 nm. (b) The matrix of excitation and emission spectra (Ex: 300–550 nm, Em: 600–780 nm).

The singlet oxygen quantum yield was measured as follows: 2 mL DMF solution containing 20 μM DPBF and 0.5 μM TMC was placed in a sealed quartz cuvette. The overall optical density of the solution was kept below 1.5, to be able to rely on the Beer–Lambert law (linear proportionality between absorbance and concentration). The laser power was 5 mW to ensure about 5% DPBF decay per 10 s irradiation interval. The experiment was repeated three times.

$$\Phi_\Delta(S) = \Phi_\Delta(R) k^S I_{aT}(R) / k^R I_{aT}(S) \quad (1)$$

$$I_a = I_0(1 - e - 2.3\mathrm{A}) \quad (2)$$

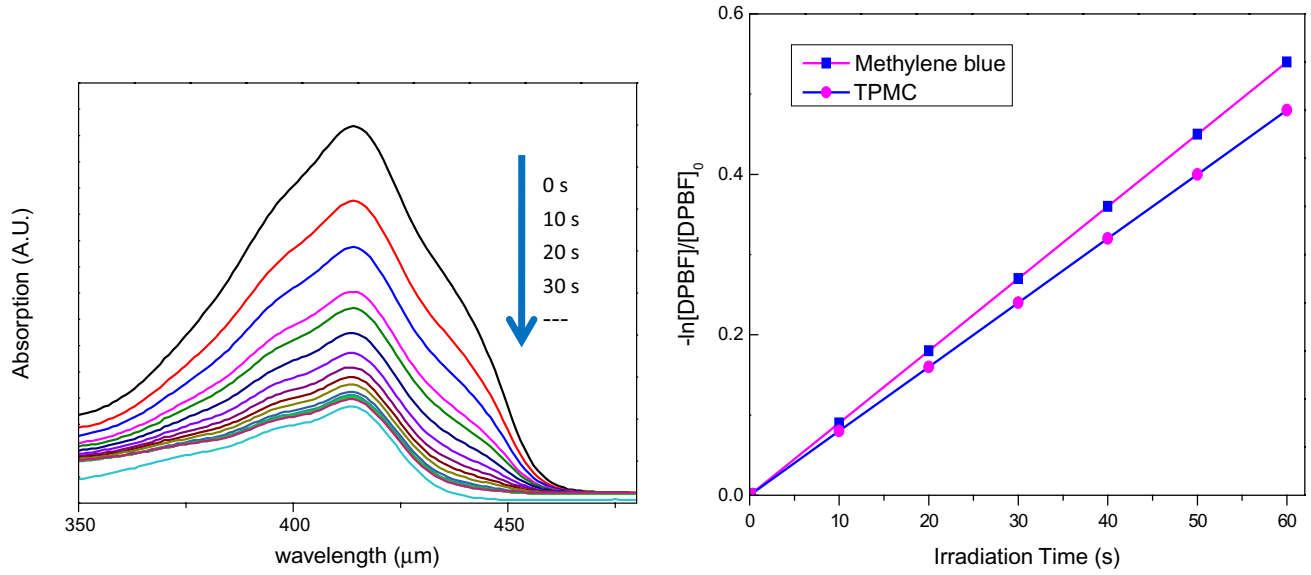

(a) (b)

Fig. 4. Photodecomposition of DPBF by $^1O_2$ after irradiation of methylene blue, TPMC in DMF (monitoring the maximum absorption of DPBF at 410 nm).

Φ_Δ was calculated on the basis of Eqs. (1) and (2).[21] Superscript S and R indicate the sample and reference compound, respectively. I_a is defined as the total amount of light absorbed by the sensitizers. A is the corresponding absorbance at irradiation wavelength. After the data were plotted as $-\ln[\text{DPBF}]/[\text{DPBF}]_0$ versus irradiation time t, straight lines were obtained for the sensitizers, and the slope for each compound was obtained after fitting with a linear function (correlation coefficient $R > 0.99946$), as shown in Fig. 4. The $^1O_2$ quantum yield (Φ_Δ) of TPMC in DMF was 48%.

3.4. *Cellular uptake of TPMC in Eca-109 and SMMC-7721 cells*

The uptake of a 5 μM solution of TPMC was measured after incubating Eca-109 and SMMC-7721 cells for different time periods in the dark. As shown in Fig. 5(a), a rapid significant uptake of

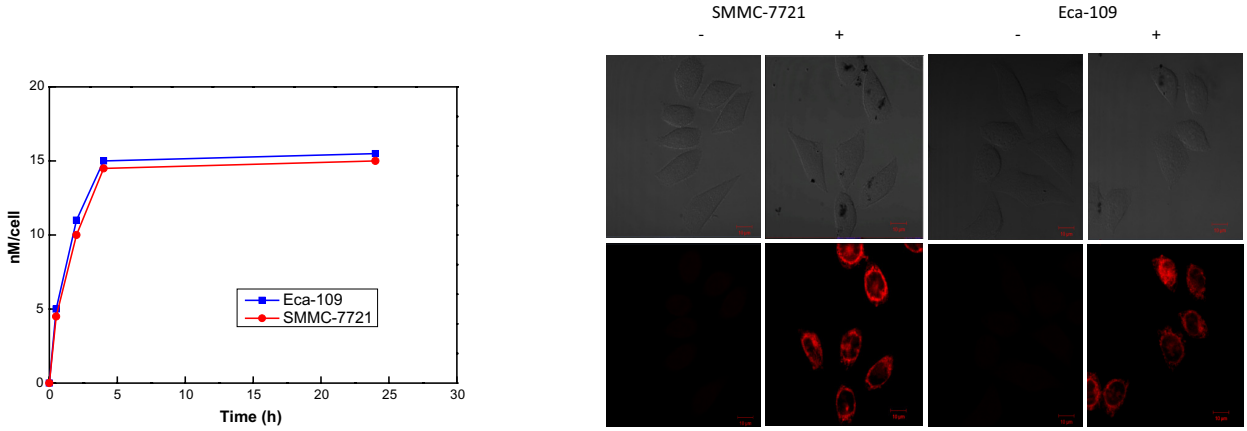

(a) (b)

Fig. 5. Time-dependent uptake of TPMC. (a) Eca-109 and SMMC-7721 cells were incubated for different time periods in the dark with a 5 μM concentration of TPMC. (b) Intracellular location of TPMC was visualized by confocal microscopy after incubating Eca-109 and SMMC-7721 cells for 24 h in the dark. The upper panel corresponds to phase contrast and lower panel to fluorescence images.

TPMC was observed after 30 min exposure, reaching a plateau after 4 h. A nucleus location of TPMC with a typical red fluorescence emission was observed by confocal microscopy after 24 h incubation by exciting at 420 nm and detecting the emission fluorescence at 656 nm [see Fig. 5(b)].

3.5. *Cell dark- and photo-toxicity*

TPMC was tested at different concentrations (2 to 10 μM) for 24 h without red light irradiation [see Fig. 6(a)]. Survival of Eca-109 and SMMC-7721 cells, as assessed by MTT assay, was greater than 80% for concentrations of 6 μM or less. When concentration was 8 μM, a slight increase in cytotoxicity was detected. However, 10 μM TPMC induced a significant amount of nonviable cells and, therefore, this concentration was not used for photo-treatments.

Figures 6(b) and 6(c) showed the changes in cell viability caused by TPMC at different concentrations and light doses, as evaluated by MTT assay. The surviving fraction of Eca-109 and SMMC-7721 cells that were exposed to light without TPMC pre-incubation was similar to that in controls (data not shown). Low light doses (1.2 J/cm^2) caused moderate damage even at the highest concentration tested. By raising the light dose to 3.6 J/cm^2, lethality over 50% was achieved but this treatment was still judged insufficient. Cell viability below 25% was observed when using TPMC at concentrations equal or less than 6 μM and at

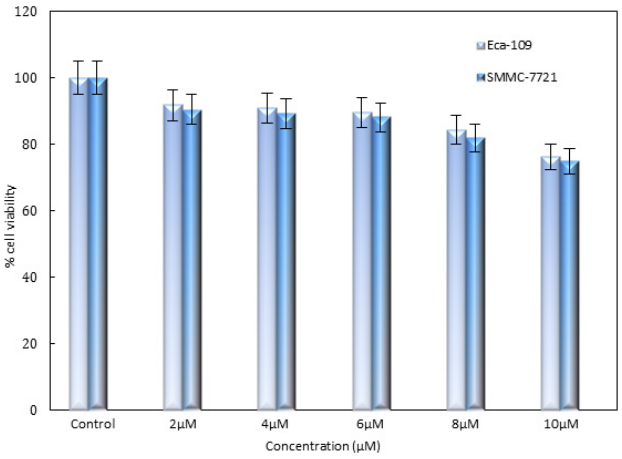

(a)

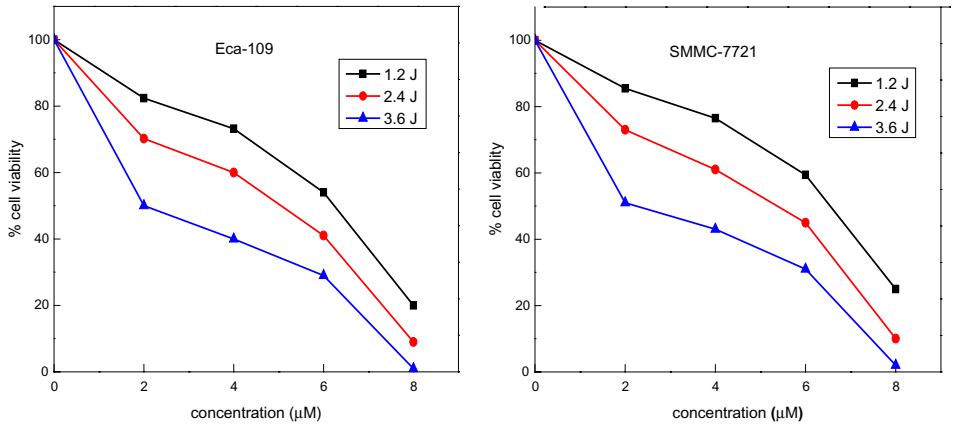

(b)

Fig. 6. (a) Dark toxicity of each concentration assayed. Data correspond to mean values ± SD from at least three different experiments. B.C) Light dose-dependent effects on cell viability after incubation with TPMC (2 to 8 μM) for 24 h, followed by irradiation. Different treatments produce significant effects on the survival of Eca-109 (b) and SMMC-7721 (c) cells. Surviving fractions of cells correspond to mean ± SD values from at least three different experiments.

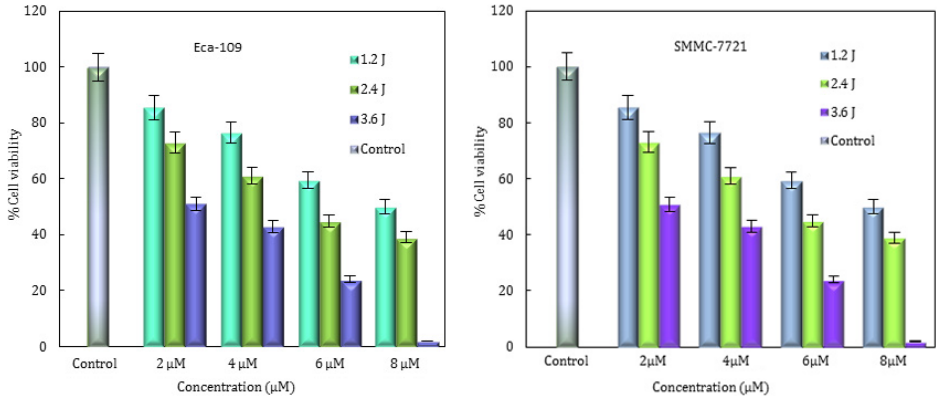

(c)

Fig. 6. (*Continued*)

maximum light dose ($3.6\,J/cm^2$), whereas treatments with $8\,\mu M$ plus $3.6\,J/cm^2$ induced lethal effect. Balance between dark toxicity and photodamage suggested that 6 or$8\,\mu M$ TPMC and $3.6\,J/cm^2$ were suitable conditions for effective photodynamic studies.

3.6. *Intracellular location of TPMC*

The nucleus location of TPMC was evaluated by confocal microscopy after incubating Eca-109 and SMMC-7721 cells for 24 h and staining them with fluorescent dye (Hoechst 33342) for cell nucleus. As shown in Fig. 7, TPMC was mainly found in the nuclear membranes and nucleus co-localized with the blue fluorescence of the nucleus probe. Thus, pink vesicles were visualized from the overlay of the red fluorescence from TPMC.

3.7. *In vivo PDT efficacy*

To determine the effects of TPMC on esophageal cancer *in vivo*, 1×10^6 Eca-109 cells were injected into the axils of nude mice to form solid tumors ($100\,mm^3$ in size). $200\,\mu L$ of $8\,\mu M$ TPMC was then injected into the tail vein and 24 h later the tumor

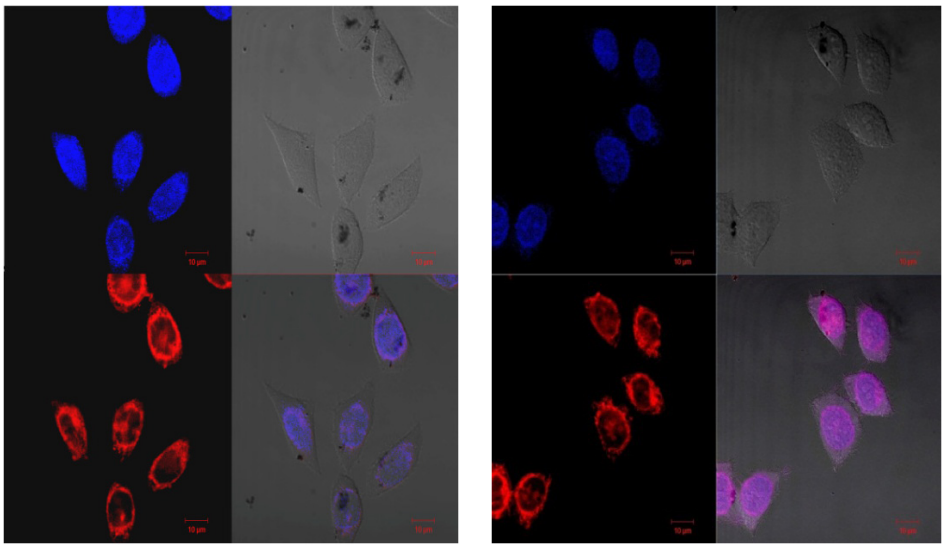

(a) (b)

Fig. 7. Intracellular localization of TPMC and staining cell nucleus. SMMC-7721 (a) and Eca-109 (b) incubated with $5\,\mu M$ of TPMC for 24 h were stained with Hoechst 33342 ($0.5\,\mu g/mL$, 30 min) and kept in the dark. Red fluorescence corresponds to TPMC and blue fluorescence represents the signal for Hoechst 33342.

was irradiated with 50 mW/cm^2 laser light for 10 min (90 J/cm^2). PDT-treated tumors began to shrink within five days and became dark, hardened and dried over the course of the next 10 days and eventually formed a scab by 20 days after treatment. The normal skin phototoxicity subsided within four days. In contrast, the tumors in control group continued to grow and were significantly larger than in PDT-treated group after 10 days post-treatment [see Fig. 8(a)]. The animals were monitored for 60 days for recurring tumor growth [see Fig. 8(b)]. TPMC-PDT gave more than 50% tumor cure.

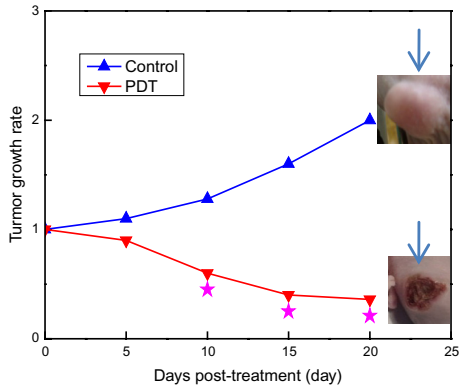

(a)

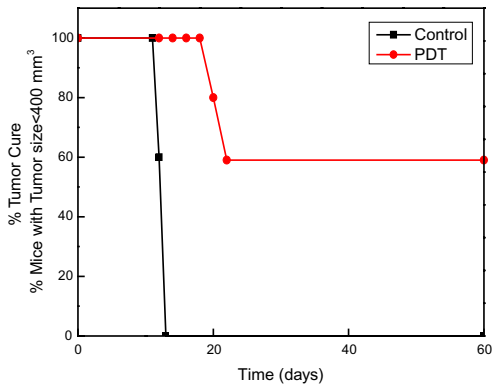

(b)

Fig. 8. *In vivo* photosensitizing efficacy of TPMC against esophageal cancer in nude mice bearing Eca-109 tumors (10 mice/group). The mice in PDT group were treated with laser light (650 nm, 90 J/cm^2) at 24 h post-injection of the drug. The control mice were not subjected to any photosensitizer or light. (a) Tumor growth rate. The tumors in control group continued to grow and were significantly larger than in PDT-treated group after 10 days post-treatment. (b) Tumor cure rate. At day 60, TPMC gave 60% tumor response (6/10 mice were tumor free).

4. Discussion

An ideal photosensitizer should have absorption spectra at long wavelengths, which allows deeper tissue penetration and decreased nonspecific lesions.[9] For instance, 630 nm light penetrates less than 0.5 cm whereas 700 nm light reaches a depth of near 0.8 cm.[22] In the present research, we show how photodynamic treatments affect cultured Eca-109 and SMMC-7721 tumor cells with chlorin derivative TPMC (see Fig. 1). Both *in vitro* and *in vivo* date supported that TPMC had the potential to be a photosensitizer for PDT.

Different wavelengths have different tissue penetrations.[9,22] TPMC may be used for the treatment of port wine stains (PWS), because of its absorption at 527 and 552 nm (see Fig. 2). PWS appears in the upper of dermis, requiring wavelengths from 488 nm to 578.2 nm (tissue penetration: 0.2 $\sim$ 0.4 cm) for treatment in PDT.[23,24] The absorption at 653 and 712 nm are suitable for deeper tumors.

Besides many photosensitizers being bright fluorophores, they also tend to emit light in the near-infrared (NIR) portion of the spectra that is useful for *in vivo* imaging.[3,25,26] Excited by 420 nm light, TPMC can emit red fluorescence at 656 nm (see Fig. 3), which means it has the prospects to become a new reagent for targeting fluorescence imaging in tumor diagnosis.[27,28]

Figure 5 demonstrated efficient uptake of TPMC by Eca-109 and SMMC-7721 cells and its relation to incubation time. Fluorescence microscopy studies using the well-known nuclear fluorescent dye (Hoechst 33342) revealed that TPMC could accumulate in nuclear membranes and nucleus (see Fig. 7). In this respect, it is already known that subcellular localization of several porphycene derivatives is heterogenous (lysosomes, mitochondria, ER, Golgi apparatus, among others), as reflected in a recent review.[29]

There are numerous *in vitro* studies assessing the effectiveness of new PSs. However, use of many different photodynamic protocols precludes comparison of the relative efficiency of new photoactivable drugs. In this regard, research carried out by Berlanda *et al.*[30] on A431 cell line with some of the most used PSs (temoporfin, hypericin, Photofrin, AlPcS4 and PPIX), provides a valuable reference for benchmarking purposes. Experimental conditions of the present work are quite similar to those of the photosensitizers mentioned above. This

includes incubation time with PS (18 versus 24 h), light fluence (1.2–3.6 J/cm^2) and time interval to perform MTT assay (24 h post-irradiation in both cases).

TPMC induced no dark toxicity in the range of concentrations used in the present photodynamic studies. Cell survival after incubation with TPMC and red-light irradiation is related to both the TPMC concentration and light dose (see Fig. 6). It showed significant concentration and light dose dependence.

In numerous PDT studies, it has been demonstrated that generation of $^1O_2$ is responsible for the initiation of cell death. The singlet oxygen was identified as ROS involved in cell photosensitization by TPMC (see Fig. 4).

PDT can induce cell death in culture by several mechanisms, including apoptosis, necrosis, mitotic catastrophe and autophagy.[31–33] Under optimal treatment conditions described above, TPMC leads to cell survival $<20\%$. When concentration was increased to 6 μM, keeping all other conditions unchanged, cell death was induced by the rupture of nuclear membrane and the damage of DNA in nucleus. In this sense, it is well accepted that high PDT doses (either high photosensitizer concentration or high light fluence or both) tend to cause cell death by necrosis, whereas PDT administered at lower doses tends to predispose cells toward apoptotic cell death.[34]

5. Conclusions

In summary, TPMC is endowed with many properties to be considered as a very good PS for PDT and photodiagnosis: It is endowed with high absorption coefficients in red spectral region ($1.67 \times 10^4 M^{-1}cm^{-1}$ at 653 nm in DMF), red fluorescence at 656 nm, high singlet oxygen quantum yield of 0.48, and is able to inactivate Eca-109 and SMMC-7721 cells with high efficiency. *In vivo*, when exposed to 650 nm laser light irradiation, Eca-109 tumors in nude mice were destroyed and a small scab was formed, 50% of tumors were cured after TPMC-PDT.

Acknowledgments

This work was supported by Chinese National Natural Science Foundation (21372042, 81301878, 81101298), Foundation of Shanghai government (13431900700, 13430722300, 13ZR1441000, 13ZR1440900), Foundation of Donghua University (No. 11D10501; 12D10515) and Foundation of Yiwu Science and Technology Bureau (2011-G1-15; 2012-G3-02).

References

1. T. J. Dougherty, C. J. Gomer, B. W. Henderson, G. Jori, D. Kessel, M. Korbelik, J. Moan, Q. Peng, "Photodynamic therapy," *J. Nat. Cancer Inst.* **90**, 889–905 (1998).
2. S. M. Fien, A. R. Oseroff, "Photodynamic therapy for non-melanoma skin cancer," *J. Nat. Compr. Canc. Netw.* **5**, 531–540 (2007).
3. J. F. Lovell, T. W. Liu, J. Chen, G. Zheng, "Activatable photosensitizers for imaging and therapy," *Chem. Rev.* **110**, 2839–2857 (2010).
4. E. A. Giuliano, I. MacDonald, D. L. McCaw, T. J. Dougherty, G. Klauss, J. Ota, J. W. Pearce, P. J. Johnson, "Photodynamic therapy for the treatment of periocular squamous cell carcinoma in horses: A pilot study," *Vet. Ophthalmol.* **11**, 27–34 (2008).
5. L. B. Josefsen, R. W. Boyle, "Photodynamic therapy and the development of metal-based photosensitisers," *Met. Based Drugs* **2008**, 276109 (2008).
6. M. Triesscheijn, P. Baas, J. H. Schellens, F. A. Stewart, "Photodynamic therapy in oncology," *Oncologist* **11**, 1034–1044 (2006).
7. J. P. Celli, B. Q. Spring, I. Rizvi, C. L. Evans, K. S. Samkoe, S. Verma, B. W. Pogue, T. Hasan, Imaging and photodynamic therapy: Mechanisms, monitoring, and optimization, *Chem. Rev.* **110**, 2795–2838 (2010).
8. Y. J. Yan, M. Z. Zheng, Z. L. Chen, X. H. Yu, X. X. Yang, Z. L. Ding, L. Xu, "Studies on preparation and photodynamic mechanism of chlorin P6-13,15-N-(cyclohexyl)cycloimide (Chlorin-H) and its antitumor effect for photodynamic therapy in vitro and in vivo," *Bioorg. Med. Chem.* **18**, 6282–6291 (2010).
9. Z. Huang, "A review of progress in clinical photodynamic therapy," *Technol. Cancer Res. Treat.* **4**, 283–293 (2005).
10. M. R. Hamblin, J. L. Miller, I. Rizvi, B. Ortel, E. V. Maytin, T. Hasan, "Pegylation of a chlorin(e6) polymer conjugate increases tumor targeting of photosensitizer," *Cancer Res.* **61**, 7155–7162 (2001).
11. R. Asano, A. Nagami, Y. Fukumoto, F. Yazama, H. Ito, I. Sakata, A. Tai, "Synthesis and biological evaluation of new chlorin derivatives as potential photosensitizers for photodynamic therapy," *Bioorg. Med. Chem.* **21**, 2298–2304 (2013).

12. J. M. Dabrowski, M. Krzykawska, L. G. Arnaut, M. M. Pereira, C. J. Monteiro, S. Simoes, K. Urbanska, G. Stochel, "Tissue uptake study and photodynamic therapy of melanoma-bearing mice with a nontoxic, effective chlorin," *ChemMedChem* **6**, 1715–1726 (2011).
13. E. Hao, E. Friso, G. Miotto, G. Jori, M. Soncin, C. Fabris, M. Sibrian-Vazquez, M. G. Vicente, "Synthesis and biological investigations of tetrakis (p-carboranylthio-tetrafluorophenyl)chlorin (TPFC)," *Org. Biomol. Chem.* **6**, 3732–3740 (2008).
14. M. Wawrzynska, W. Kalas, D. Bialy, E. Ziolo, J. Arkowski, W. Mazurek, L. Strzadala, "In vitro photodynamic therapy with chlorin e6 leads to apoptosis of human vascular smooth muscle cells," *Arch. Immunol. Ther. Exp.* **58**, 67–75 (2010).
15. V. A. Ol'shevskaya, R. G. Nikitina, A. N. Savchenko, M. V. Malshakova, A. M. Vinogradov, G. V. Golovina, D. V. Belykh, A. V. Kutchin, M. A. Kaplan, V. N. Kalinin, V. A. Kuzmin, A. A. Shtil, "Novel boronated chlorin e6-based photosensitizers: Synthesis, binding to albumin and antitumour efficacy," *Bioorg. Med. Chem.* **17**, 1297–1306 (2009).
16. H. B. Ris, H. J. Altermatt, B. Nachbur, C. M. Stewart, Q. Wang, C. K. Lim, R. Bonnett, U. Althaus, "Intraoperative photodynamic therapy with m-tetrahydroxyphenylchlorin for chest malignancies," *Lasers Surg. Med.* **18**, 39–45 (1996).
17. J. Svensson, A. Johansson, S. Grafe, B. Gitter, T. Trebst, N. Bendsoe, S. Andersson-Engels, K. Svanberg, "Tumor selectivity at short times following systemic administration of a liposomal temoporfin formulation in a murine tumor model," *Photochem. Photobiol.* **83**, 1211–1219 (2007).
18. N. Dragicevic-Curic, S. Grafe, B. Gitter, A. Fahr, "Efficacy of temoporfin-loaded invasomes in the photodynamic therapy in human epidermoid and colorectal tumour cell lines," *J. Photochem. Photobiol. B, Biol.* **101**, 238–250 (2010).
19. J. A. Howard, "The new wilderness," *J. Am. Coll. Dent.* **43**, 15–22 (1976).
20. Y. A. Cheng, C. S. A, J. D. Meyers, I. Panagopoulos, B. Fei, C. Burda, "Highly efficient drug delivery with gold nanoparticle vectors for in vivo photodynamic therapy of cancer," *J. Am. Chem. Soc.* **130**, 10643–10647 (2008).
21. P. Zimcik, M. Miletin, K. Kopecky, Z. Musil, P. Berka, V. Horakova, H. Kucerova, J. Zbytovska, D. Brault, "Influence of aggregation on interaction of lipophilic, water-insoluble azaphthalocyanines with DOPC vesicles," *Photochem. Photobiol.* **83**, 1497–1504 (2007).
22. J. C. Finlay, S. Mitra, M. S. Patterson, T. H. Foster, "Photobleaching kinetics of Photofrin in vivo and in multicell tumour spheroids indicate two simultaneous bleaching mechanisms," *Phys. Med. Biol.* **49**, 4837–4860 (2004).
23. Y. Wang, Z. Zuo, Y. Gu, N. Huang, R. Chen, B. Li, H. Qiu, J. Zeng, J. Zhu, J. Liang, "New optional photodynamic therapy laser wavelength for infantile port wine stains: 457 nm," *J. Biomed. Opt.* **17**, 068003 (2012).
24. A. V. Evans, A. Robson, R. J. Barlow, H. A. Kurwa, "Treatment of port wine stains with photodynamic therapy, using pulsed dye laser as a light source, compared with pulsed dye laser alone: A pilot study," *Lasers Surg. Med.* **36**, 266–269 (2005).
25. W. W. Chin, P. S. Thong, R. Bhuvaneswari, K. C. Soo, P. W. Heng, M. Olivo, "In-vivo optical detection of cancer using chlorin e6–polyvinylpyrrolidone induced fluorescence imaging and spectroscopy," *BMC Med. Imaging* **9**, 1 (2009).
26. M. R. Hamblin, M. Rajadhyaksha, T. Momma, N. S. Soukos, T. Hasan, "In vivo fluorescence imaging of the transport of charged chlorin e6 conjugates in a rat orthotopic prostate tumour," *Br. J. Cancer* **81**, 261–268 (1999).
27. E. F. Silva, F. A. Schaberle, C. J. Monteiro, J. M. Dabrowski, L. G. Arnaut, "The challenging combination of intense fluorescence and high singlet oxygen quantum yield in photostable chlorins — a contribution to theranostics," *Photochem. Photobiol. Sci.* **12**, 1187–1192 (2013).
28. K. Stefflova, H. Li, J. Chen, G. Zheng, "Peptide-based pharmacomodulation of a cancer-targeted optical imaging and photodynamic therapy agent," *Bioconjug. Chem.* **18**, 379–388 (2007).
29. J. C. Stockert, M. Canete, A. Juarranz, A. Villanueva, R. W. Horobin, J. I. Borrell, J. Teixido, S. Nonell, "Porphycenes: Facts and prospects in photodynamic therapy of cancer," *Curr. Med. Chem.* **14**, 997–1026 (2007).
30. J. Berlanda, T. Kiesslich, V. Engelhardt, B. Krammer, K. Plaetzer, "Comparative in vitro study on the characteristics of different photosensitizers employed in PDT," *J. Photochem. Photobiol. B Biol.* **100**, 173–180 (2010).
31. E. Buytaert, M. Dewaele, P. Agostinis, "Molecular effectors of multiple cell death pathways initiated by photodynamic therapy," *Biochim. Biophys. Acta* **1776**, 86–107 (2007).
32. S. Rello-Varona, J. C. Stockert, M. Canete, P. Acedo, A. Villanueva, "Mitotic catastrophe induced in HeLa cells by photodynamic treatment with Zn(II)-phthalocyanine," *Int. J. Oncology* **32**, 1189–1196 (2008).
33. M. Dewaele, T. Verfaillie, W. Martinet, P. Agostinis, "Death and survival signals in photodynamic therapy," *Methods Mol. Biol.* **635**, 7–33 (2010).

34. P. Mroz, A. Yaroslavsky, G. B. Kharkwal, M. R. Hamblin, "Cell death pathways in photodynamic therapy of cancer," *Cancers* **3**, 2516–2539 (2011).
35. M. C. Alley, D. A. Scudiero, A. Monks, M. L. Hursey, M. J. Czerwinski, D. L. Fine, B. J. Abbott, J. G. Mayo, R. H. Schoemaker, M. R. Boyd, "Feasibility of drug screening with panels of human tumor cell lines using a microculture tetrazolium assay," *Cancer Res.* **48**, 589–560 (1988).